Energy Dependence of Higher Moments of Net-proton Multiplicity Distributions at STAR

Xiaofeng Luo（罗晓峰）

Institute of Particle Physics,
Central China Normal University

Feb. 20, 2014

STAR Collaboration, Phys. Rev. Lett. 112, 032302 (2014)

Outline

- Introduction
- Analysis Techniques
- Results and Discussion
- Summary

Exploring the Phase Diagram of QCD Matter

1 T_{ini}, T_C ***LHC***, ***RHIC***

2 T_E ***RHIC***, ***SPS***, ***FAIR***

3 **Phase boundary** ***RHIC***, ***FAIR***, ***CSR***

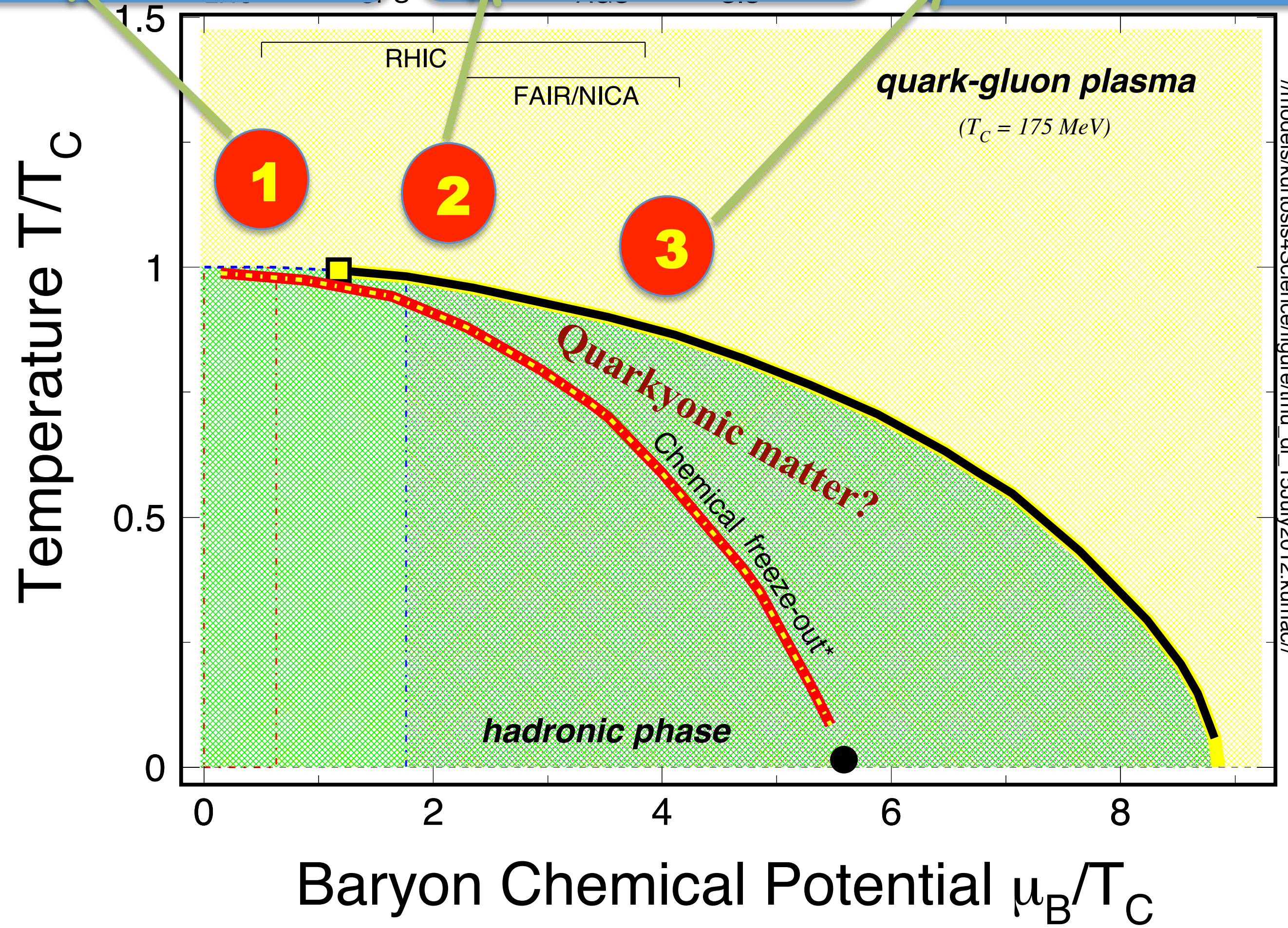

RHIC (Relativistic Heavy Ion Collider)

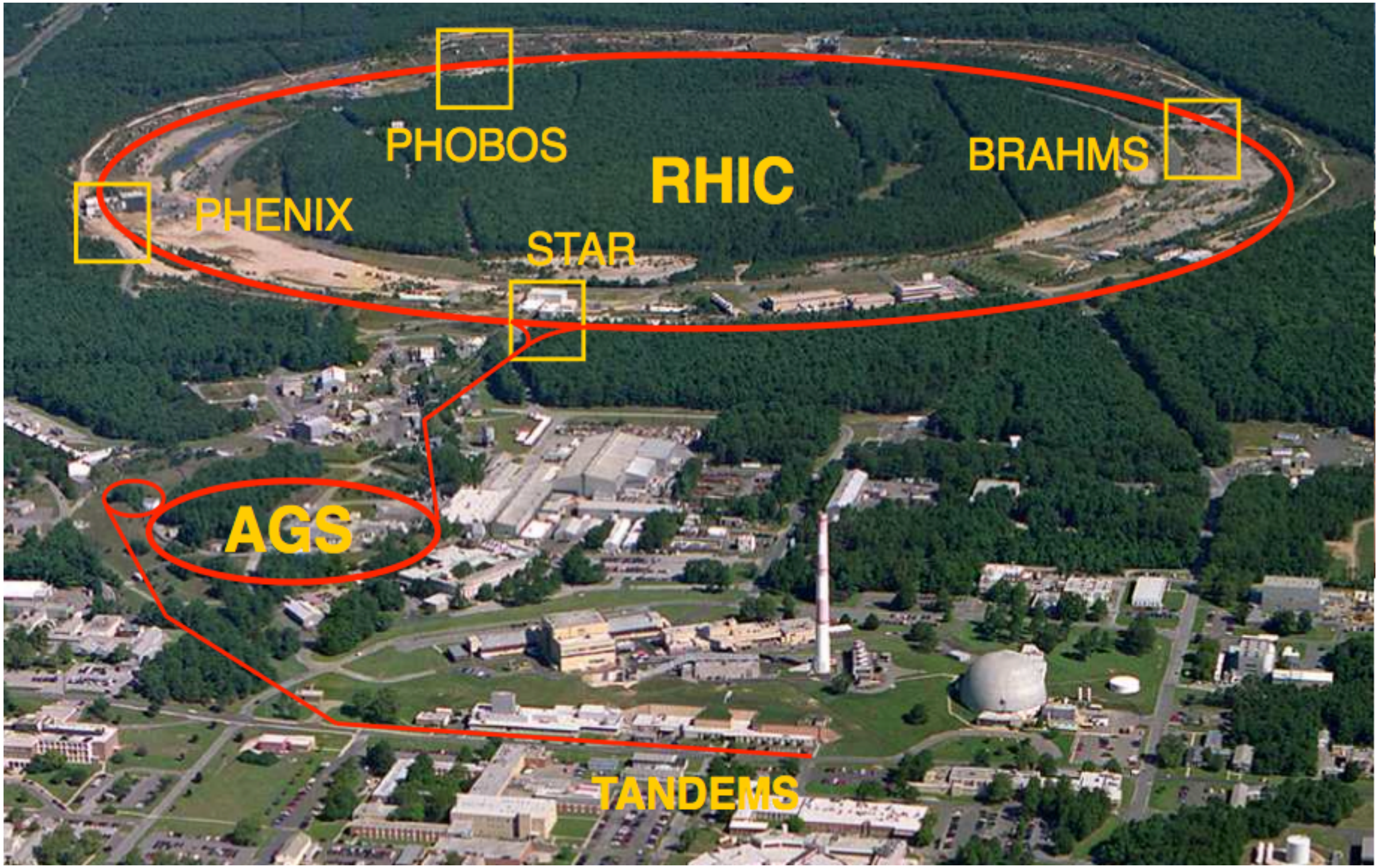

The high energy heavy-ion collider $\sqrt{s}$ = 200 - 5 GeV
The highest energy polarized proton collider (500 GeV)

STAR Detector

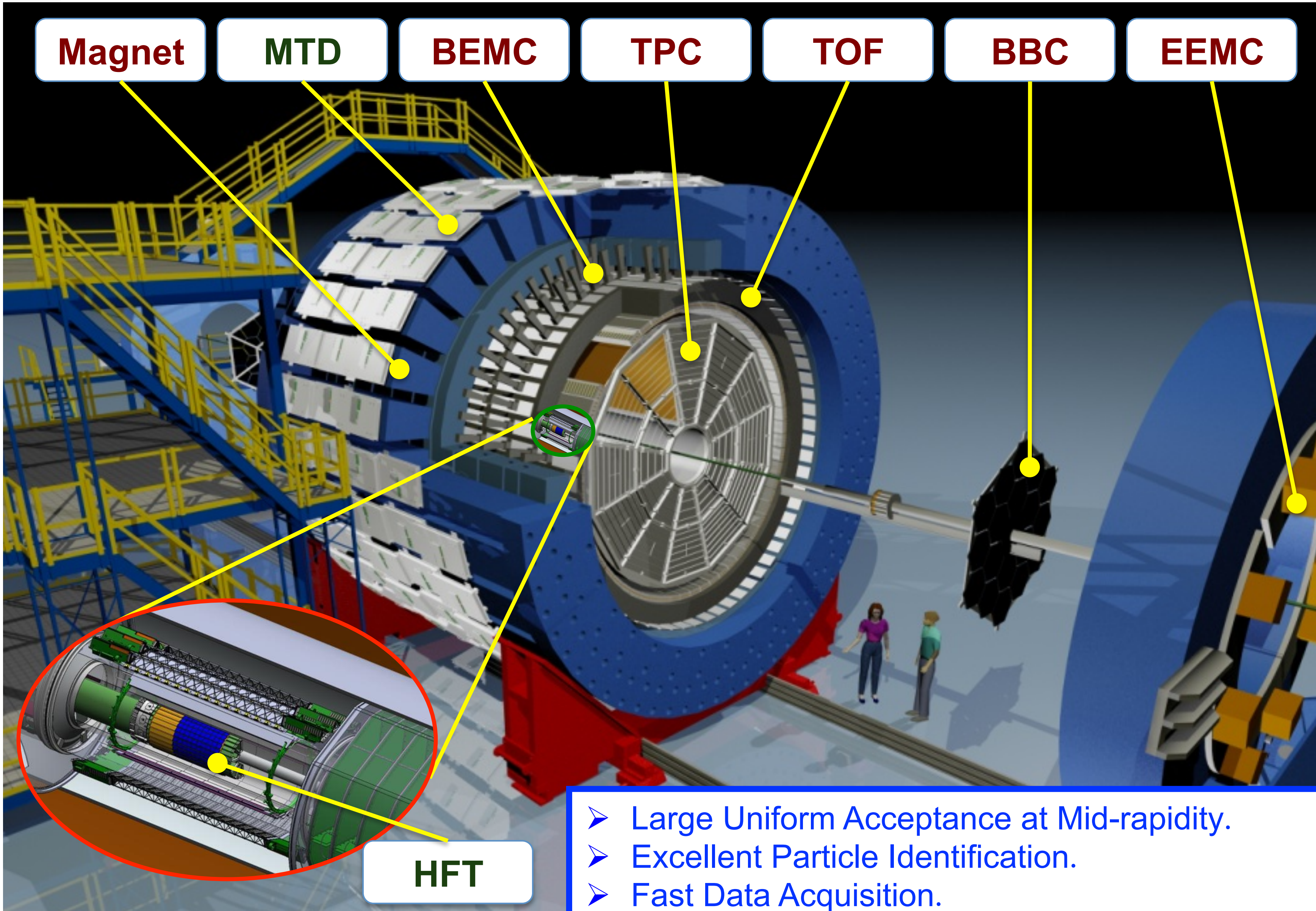

- Large Uniform Acceptance at Mid-rapidity.
- Excellent Particle Identification.
- Fast Data Acquisition.

RHIC Beam Energy Scan–Phase I

In the first phase of the RHIC Beam Scan (BES), seven energies were surveyed in 2010 and 2011.

√s (GeV)	μ_B (MeV)	Events (Million)
7.7	422	4
11.5	316	12
19.6	206	36
27	156	70
39	112	130
62.4	73	67
200	24	240

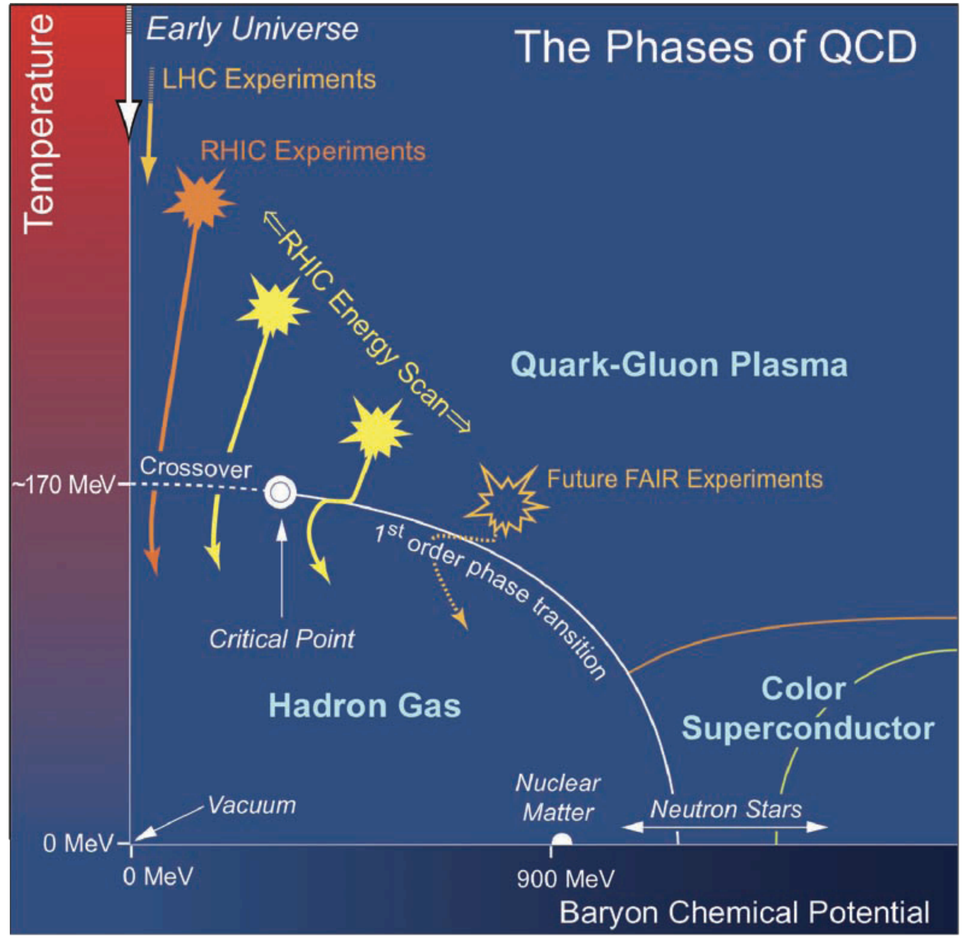

The main goals of BES program:

- **Turn-off of QGP signatures.**
- **Search for QCD critical point.**
- **Map the first order phase transition.**

Search for the QCD Critical Point

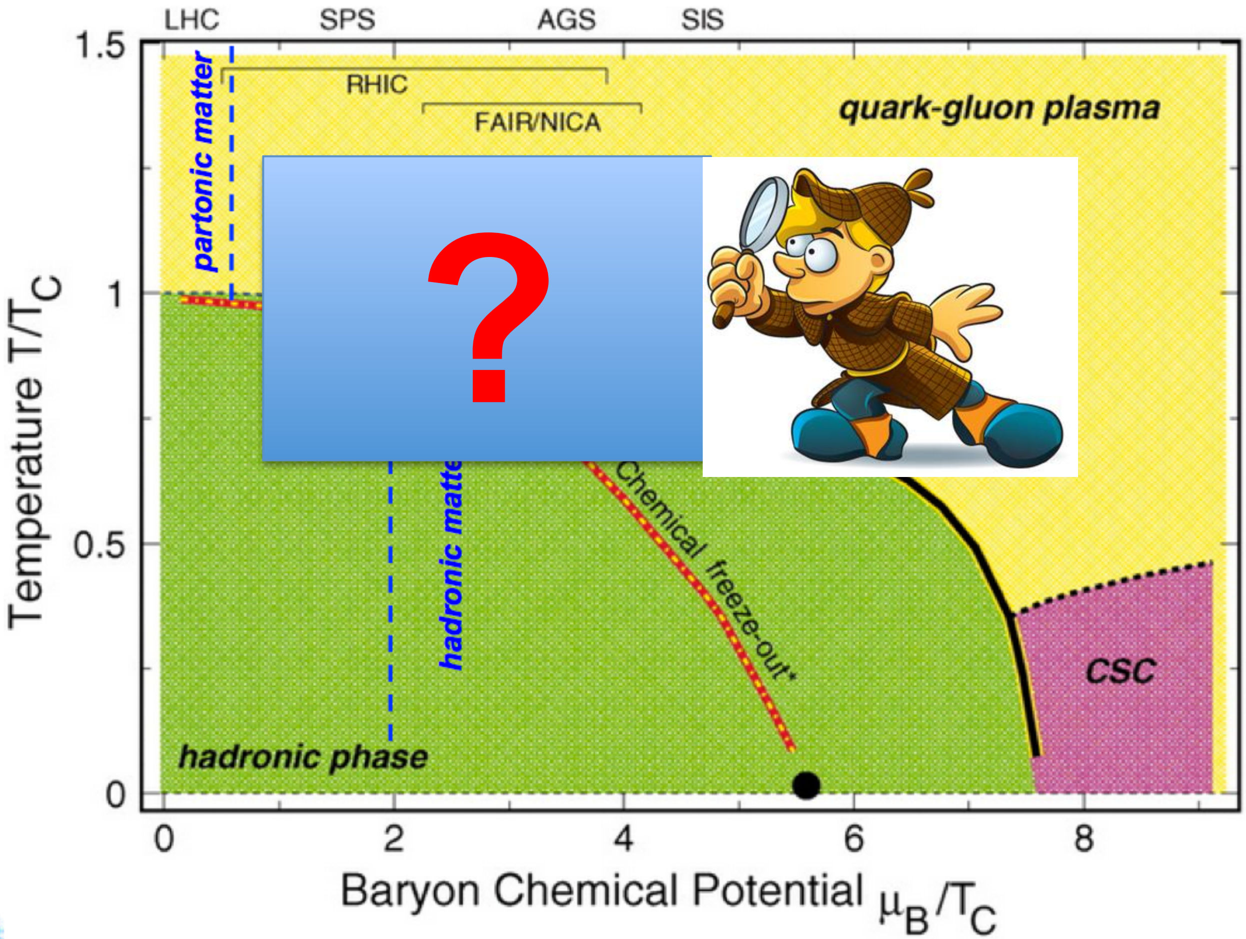

Theory：Lattice QCD et al.
Experiment：HIC et al.

S. Gupta, 罗晓峰, B. Mohanty, H.G. Ritter, and 许怒,
Science, 332, 1525 (2011).

Experimental confirmation of QCD Critical Point is an excellent test of QCD theory in the non-perturbative region and is the milestone of exploring the QCD Phase Diagram.

Critical Point

T. Andrews.
Phil. Trans. Royal Soc., 159:575, 1869.

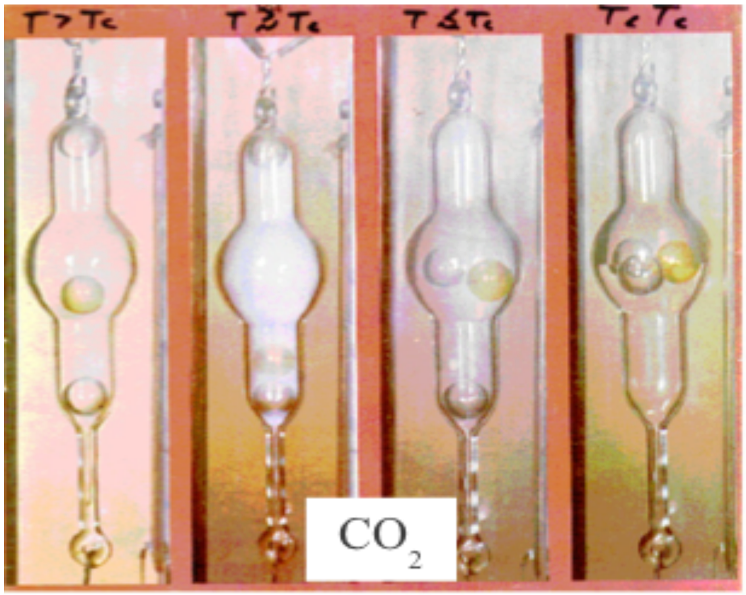

Critical Opalescence as observed in CO2 liquid-gas transition.

At the Critical Point (CP):

- 2nd order Phase Transition.
- Diverges of the thermodynamics quantities, such as correlation length (ξ), Susceptibilities (χ), heat capacity (C_V).
- light wavelength comparable with the correlation length: Critical Opalescence.
- Universality Class: QCD critical point has the same critical exponents as liquid-gas critical point (Z_2 Class).
- Critical slowing down, finite size effects et al.

QCD Critical Point Search: Strategy

- Need sensitive observable.
- Search for the non-monotonic dependence on energy.
- Understand the non-CP physics effect.
- Comparing with the QCD based dynamical model.

Characteristic Signature of Critical Point：
Non-monotonic dependence on colliding energy.

Higher Moments (I): Sensitive to the Correlation Length

Skewness:

C_n: n^{th} order cumulants

$$S = \frac{C_{3,N}}{(C_{2,N})^{3/2}} = \frac{<(N-<N>)^3>}{\sigma^3}$$

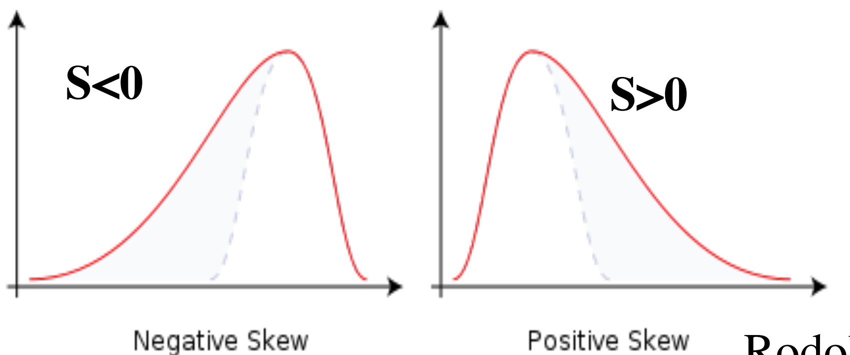

Rodolfo Hermans

Kurtosis:

$$\kappa = \frac{C_{4,N}}{(C_{2,N})^2} = \frac{<(N-<N>)^4>}{\sigma^4} - 3$$

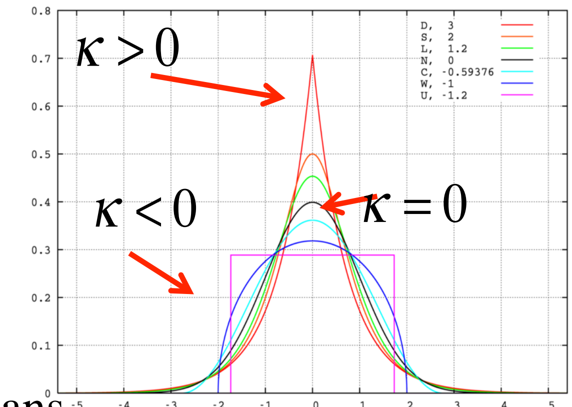

- Ideal probe of non-gaussian fluctuations.
- Sensitive to the correlation length (ξ).

$$< (\delta N)^2 > \sim \xi^2 \qquad < (\delta N)^3 > \sim \xi^{4.5}$$

$$< (\delta N)^4 > - \ 3 < (\delta N)^2 >^2 \sim \xi^7$$

M. A. Stephanov,
Phys. Rev. Lett. 102, 032301 (2009);
Phys. Rev. Lett. 107, 052301 (2011);

Search for CP in Heavy Ion Collisions (ξ~2-3 fm)

Higher Moments (II): Related to the Susceptibility

Pressure: $\frac{p}{T^4} = \frac{1}{VT^3}\ln Z(V,T,\mu_B,\mu_Q,\mu_S)$

Susceptibility:

$$\chi_q^{(n)} = \frac{\partial^n (p/T\wedge 4)}{\partial(\mu_q)^n}, q = B,Q,S$$

(Conserved Quantum Number)

$$\chi_q^{(1)} = \frac{1}{VT^3}\langle \delta N_q \rangle,$$

$$\chi_q^{(2)} = \frac{1}{VT^3}\left\langle (\delta N_q)^2 \right\rangle$$

$$\chi_q^{(3)} = \frac{1}{VT^3}\left\langle (\delta N_q)^3 \right\rangle$$

$$\chi_q^{(4)} = \frac{1}{VT^3}\left(\left\langle (\delta N_q)^4 \right\rangle - 3\left\langle (\delta N_q)^2 \right\rangle^2\right)$$

Lattice QCD

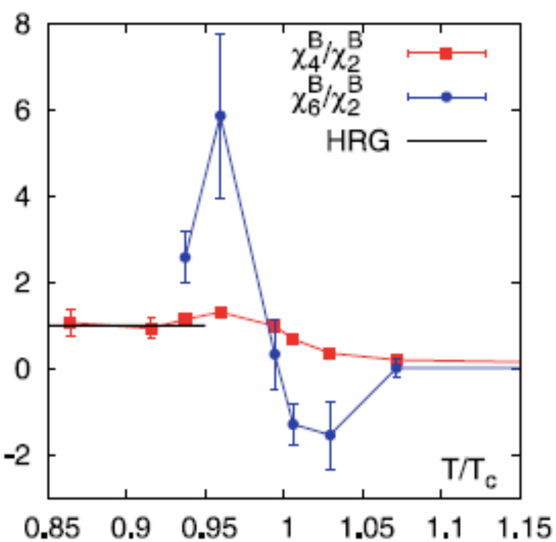

- **Susceptibility ⇔ Moments/Cumulants**

$$\boxed{\kappa\sigma^2 \sim \frac{\chi^{(4)}}{\chi^{(2)}}, S\sigma \sim \frac{\chi^{(3)}}{\chi^{(2)}}, \frac{\sigma^2}{M} \sim \frac{\chi^{(2)}}{\chi^{(1)}}}$$

R.V. Gavai and S. Gupta, *PLB 696, 459 (2011).*
S. Gupta, et al., *Science, 332, 1525(2011).*
Y. Hatta, et al, *PRL. 91, 102003 (2003).*
A. Bazavov et al *.arXiv::1208.1220. 1207.0784.*
F. Karsch et al, PLB 695, 136 (2011).

Experimental Measurement

Event-by-event fluctuations of net-baryon (B), net-charge (C) and net-strangeness number (S).

STAR , Xiaofeng Luo et al; *PRL105, 022302(2010).*

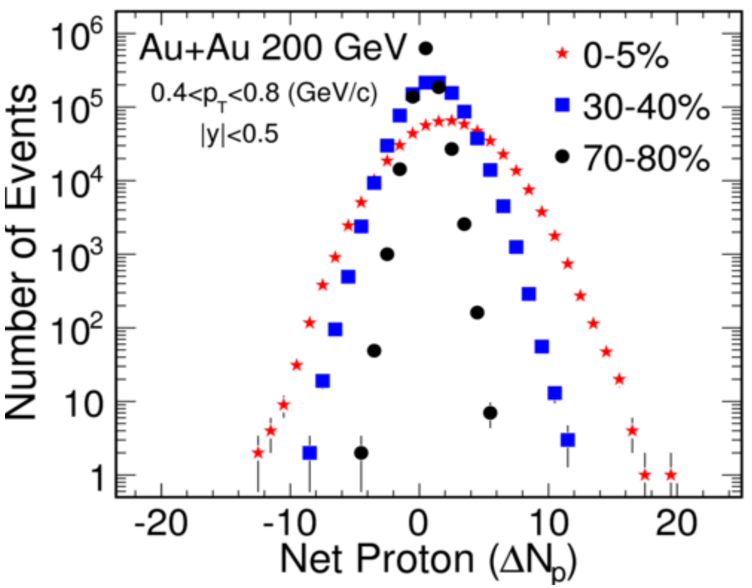

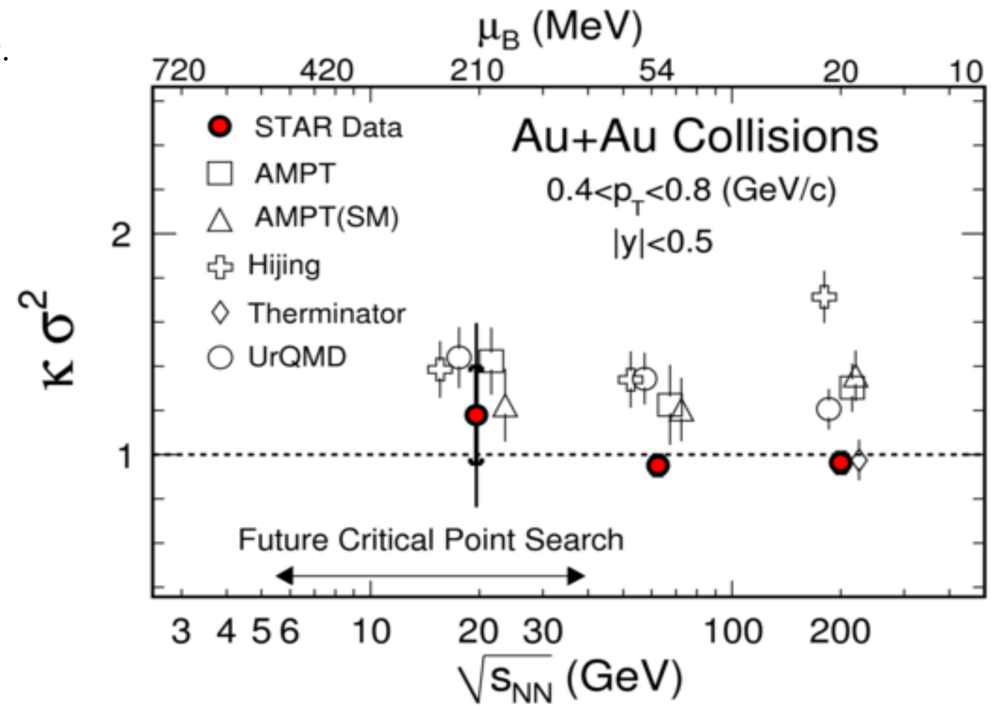

- ➢ First measurement of the higher moments of net-proton distributions at RHIC.
- ➢ There has no evidence for the existence of QCD critical point at μ_B <200 MeV.

Event and Track Selection

Energy (GeV)	7.7	11.5	19.6	27	39	62.4	200
Statistics (Million), 0-80%	~3	~6.6	~15	~30	~87	~47	~238
Year	2010	2010	2011	2011	2010	2010	2010

- Events QA: Some quality cuts have been applied. (Bad Run/Events Removed)
- PID : Energy loss (dE/dx) in STAR TPC is used to identify protons with high purity within $0.4<p_T<0.8$ (GeV/c) and at mid-rapidity $|y|<0.5$.

$$Z_p = \frac{\ln((dE/dx)_{exp.}/(dE/dx)_{theory})}{\sigma_{TPC}}$$

STAR TPC dE/dx PID

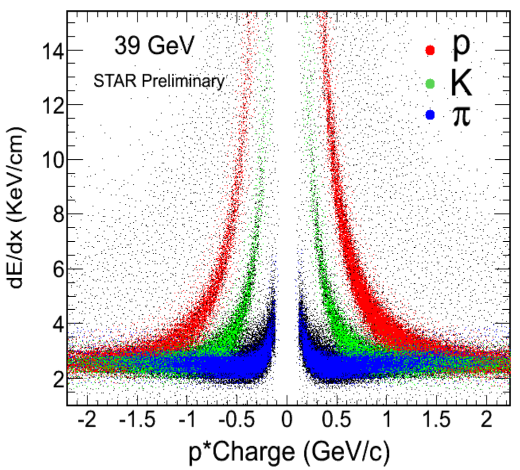

$$|Z_p| < 2$$

Proton Phase Space

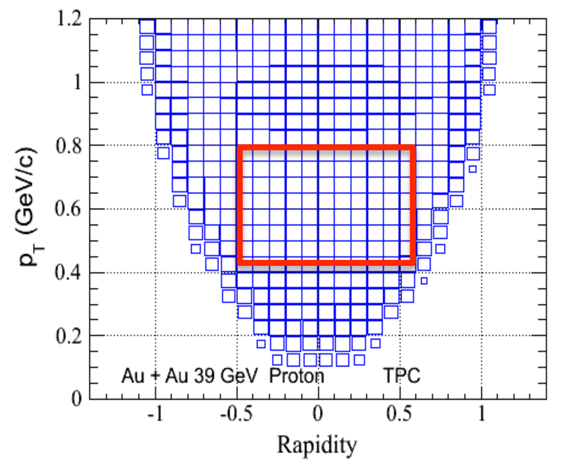

Analysis Techniques

Techniques:

Background/artifacts effects.

- Auto-correlation effects.
- Volume fluctuation effects.
- Detector efficiency effects.

Initial volume fluctuation

Volume flu. within centrality

1. Define the centrality without p and pbar
2. Define the centrality with large η window.
3. Centrality Bin Width Correction (CBWC).
4. Efficiency Correction

X. Luo (STAR Collaboration), J. Phys. Conf. Ser. 316, 012003 (2011). (CBWC)
X. Luo (STAR Collaboration), Nucl. Phys. A 904, 911c (2013).
X. Luo (STAR Collaboration), Pos (CPOD 2013) 019 [arXiv: 1306.3106]. (Initial volume fluctuation)
X. Luo, J. Phys. G 39, 025008 (2012). (Statistical Error)
X. Luo, J. Xu, B. Mohanty, N. Xu, J. Phys. G 40, 105104 (2013). (Volume flu. and auto-correlation)

Centrality Definition

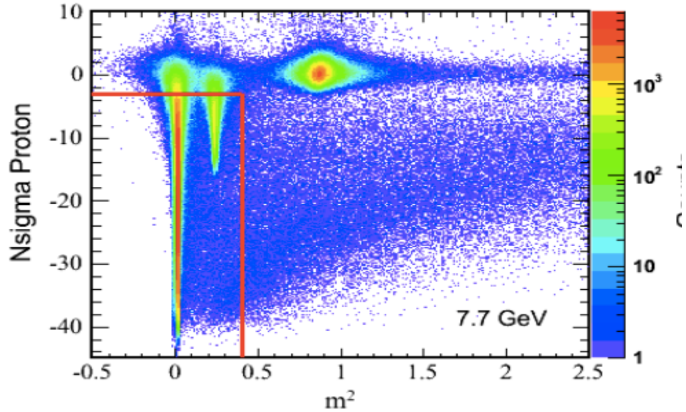

Refmult3 (Charged Pion+Kaon)

To avoid auto-correlation.

|η|<1, Current TPC Acceptance Limit.

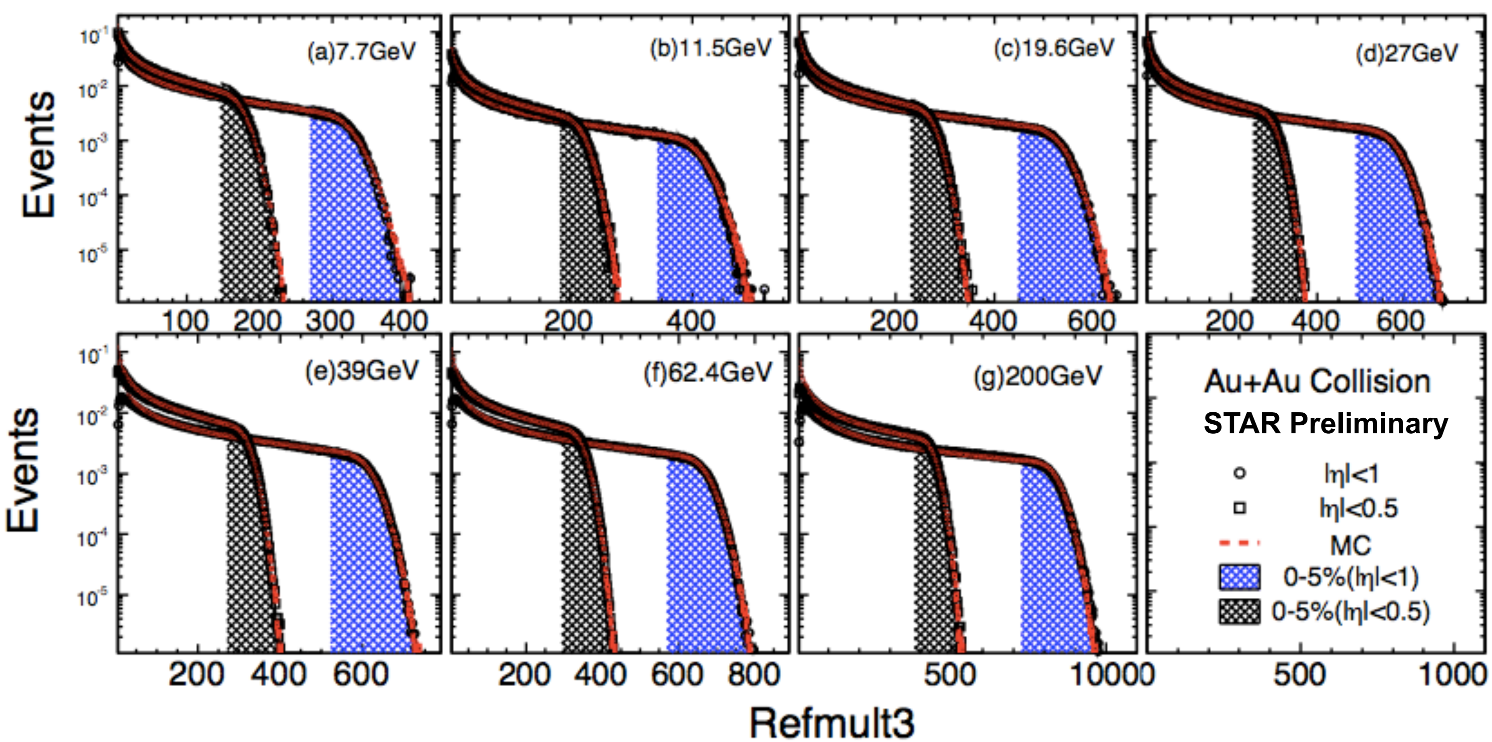

Centrality Bin Width Effect and Correction

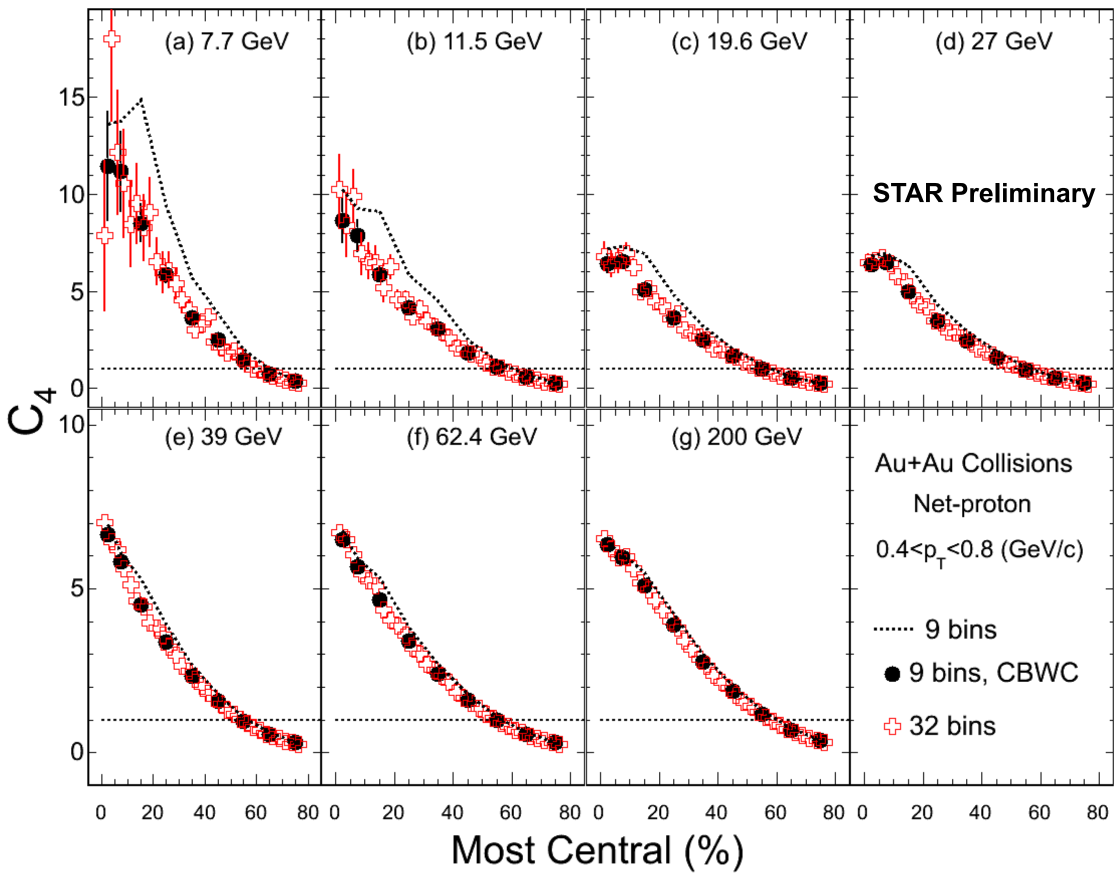

CBWC: $\omega_r = \frac{n_r}{\sum n_r}$

$$(1): C_2 = \sum_{r=1}^{N} \omega_r C_{2,r}$$

$$(2): C_3 = \sum_{r=1}^{N} \omega_r C_{3,r}$$

$$(3): C_4 = \sum_{r=1}^{N} \omega_r C_{4,r}$$

r: r^{th} multiplicity.

n_r: # of events in r.

1. The trend are different with different bin width.
2. Low energy has larger effects.
3. Volume fluctuations within one centrality bin will enlarge the cumulants.

Centrality Resolution Effect

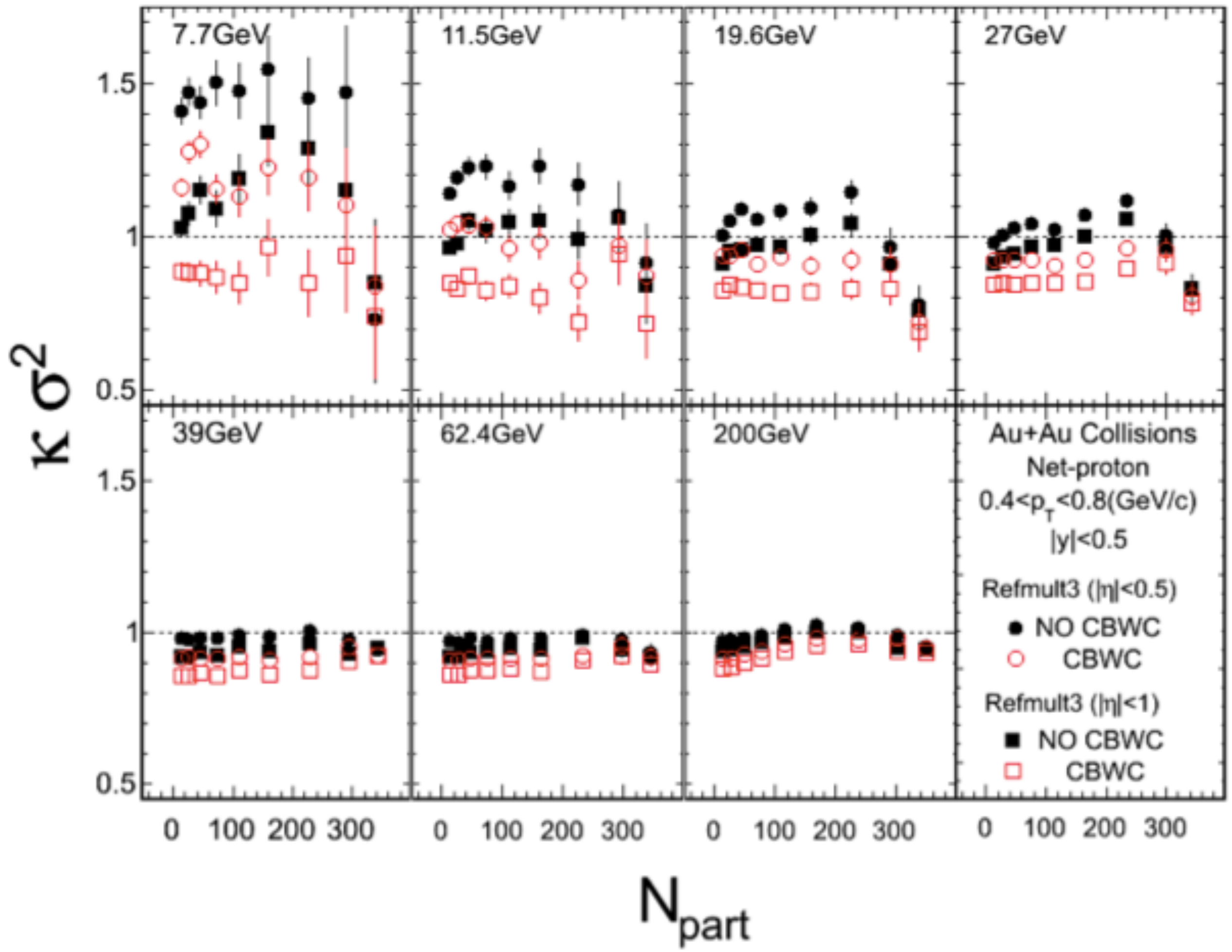

➢ Large difference are observed in mid-central /peripheral and low energies for different Refmult3 definition (different centrality resolutions).

Detector Efficiency Correction: Binomial Efficiency

This correction is done for refmult3 by refmult3 and corrected for bin width after efficiency correction. 5% uncertainty on the efficiency number is considered.

$$C_2(X-Y)=\frac{C_2(x-y)+(\varepsilon-1)(\langle x\rangle+\langle y\rangle)}{\varepsilon^2}$$

$$C_3(X-Y)=\frac{C_3(x-y)+3(\varepsilon-1)(C_2(x)-C_2(y))+(\varepsilon-1)(\varepsilon-2)(\langle x\rangle-\langle y\rangle)}{\varepsilon^3}$$

X: Input Proton,
Y: Input Anti-proton,
x: measured proton
y: measured anti-proton
C_2, C_3, C_4: 2nd, 3rd 4th order cumulants.

$$\varepsilon=\frac{\varepsilon_p+\varepsilon_{\bar{p}}}{2}$$

$$C_4(X-Y)=\frac{C_4(x-y)-2(\varepsilon-1)C_3(x+y)+8(\varepsilon-1)(C_3(x)+C_3(y))+(5-\varepsilon)(\varepsilon-1)C_2(x+y)+8(\varepsilon-2)(\varepsilon-1)(C_2(x)+C_2(y))+(\varepsilon^2-6\varepsilon+6)(\varepsilon-1)(\langle x\rangle+\langle y\rangle)}{\varepsilon^4}$$

Average Efficiency within transverse momentum range (a,b): Embedding efficiency weighted by p_T spectra.

$$\varepsilon(p\ \ or\ \ \bar{p})=\frac{\int_a^b \varepsilon'(p_T)f(p_T)p_T\,\mathrm{dp_T}}{\int_a^b f(p_T)p_T\,\mathrm{dp_T}}$$

$\varepsilon'(p_T)$: embedding p_T dependent efficiency for proton or anti-proton.

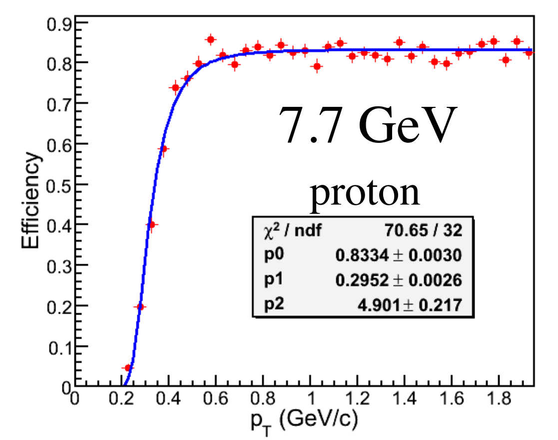

Error Estimation Method

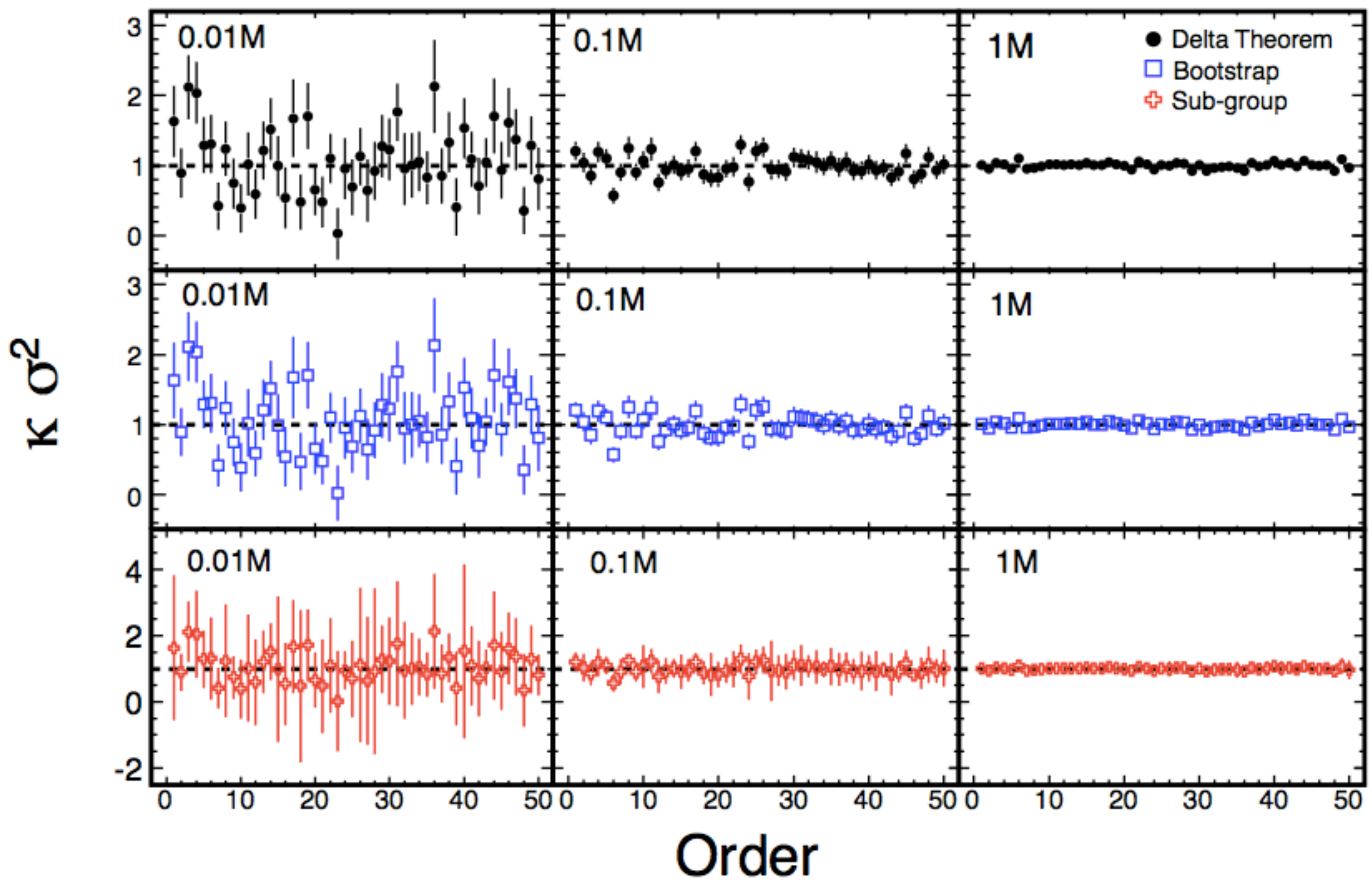

Delta theorem and Bootstrap method give reasonable error estimation
While the sub-group method overestimate the statistical errors.

Experimental Results

Raw Event-by-Event Net-proton Distributions

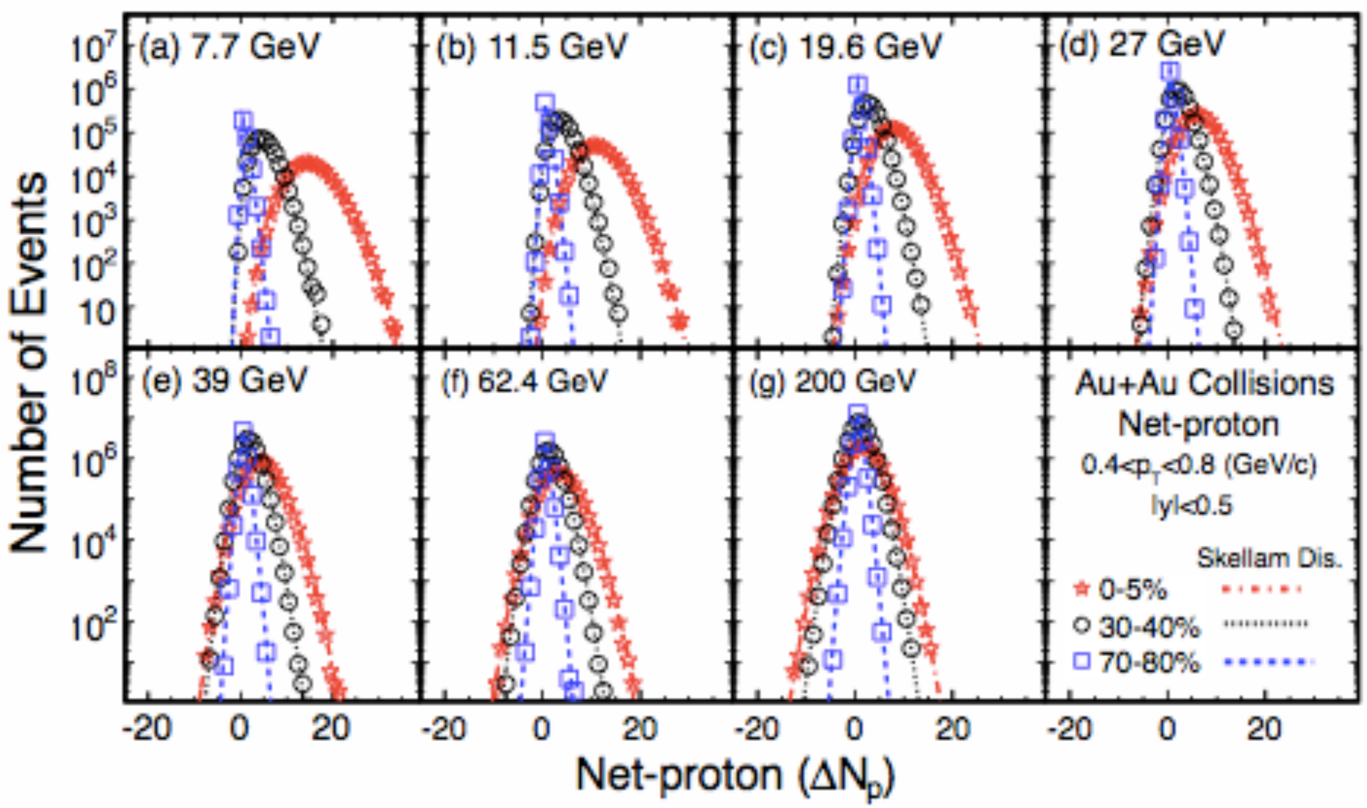

The raw net-p distributions are only for illustration purpose and should not be used to calculate the net-proton moments. (the centrality bin width correction have to be applied).

Mean net-proton, proton and anti-proton

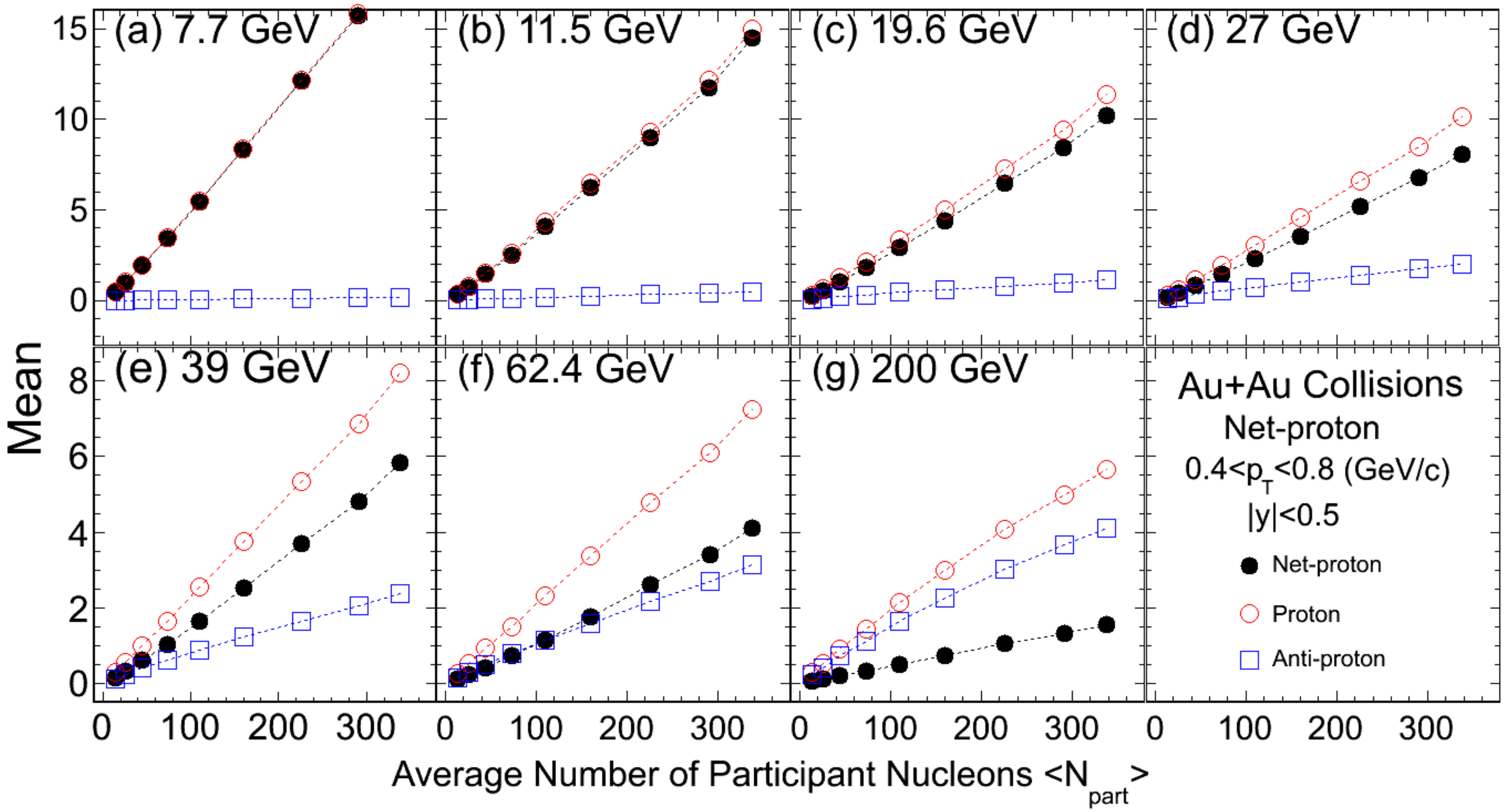

- Net-proton, proton and anti-proton number increase with N_{part}.
- Net-proton increase when energy decrease and dominated by proton at low energies. (Interplay between baryon stopping and pair production)

Centrality Dependence of Net-proton Cumulants

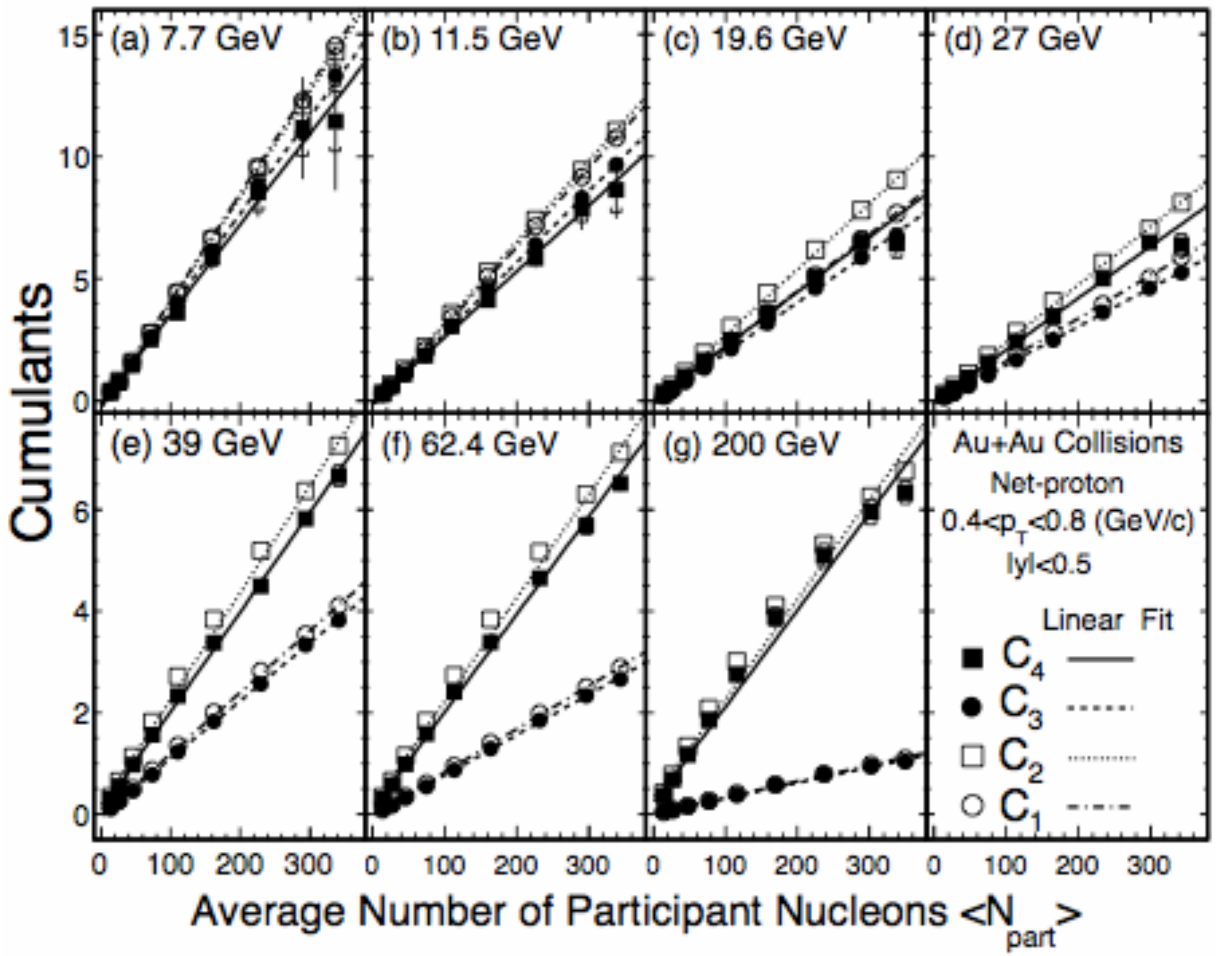

- Linear increase with N_{part}.
- C1~C3 and C2~C4 for all energies.

Baselines

- If proton and anti-proton are independent， then

Net-proton: $$C_n(p-\overline{p}) = C_n(p) + (-1)^n C_n(\overline{p}), \qquad n = 1,2,3\ldots$$

1. Poisson Baseline: Assuming that the proton and anti-proton are independent distributed as Poisson distribution.

Then $$C_n(X) = \langle X \rangle, \qquad X = p \;, \; \overline{p}$$

2. Binomial Baseline: Assuming that the proton and anti-proton are independent distributed as Binomial distribution.

Mean: μ=<X>
Variance to mean ratio: $\varepsilon=\sigma^2/\mu$

$$C_2(X) = \sigma^2 = \varepsilon\mu \qquad C_3(X) = S\sigma^3 = \varepsilon\mu(2\varepsilon - 1)$$

$$C_4(X) = \kappa\sigma^4 = \varepsilon\mu(6\varepsilon^2 - 6\varepsilon + 1) \qquad X = p \;, \; \overline{p}$$

3. Models： HRG， UrQMD， AMPT， Hijing etc.

Baseline (I) : Poisson and Binomial

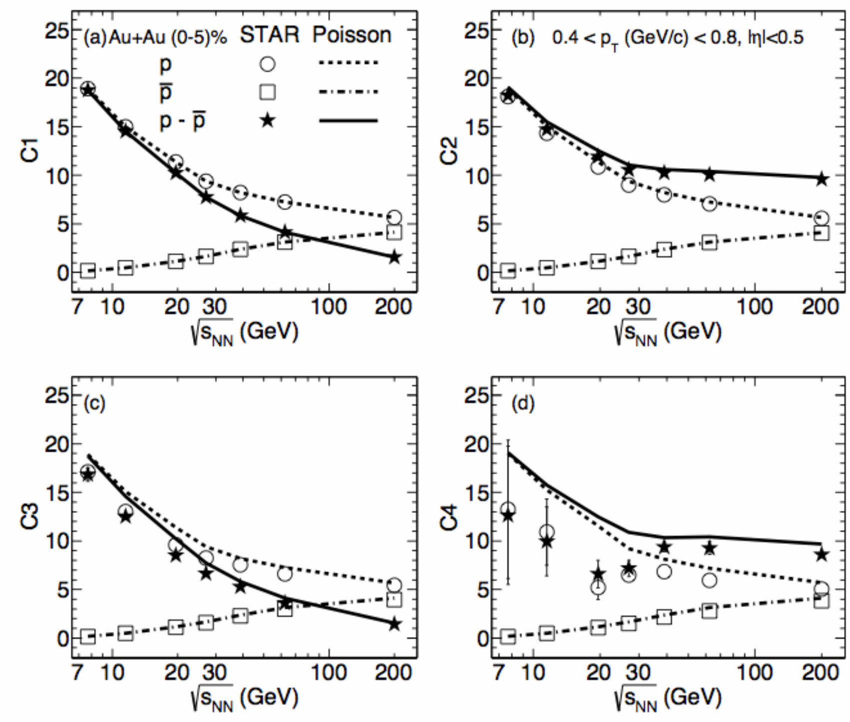

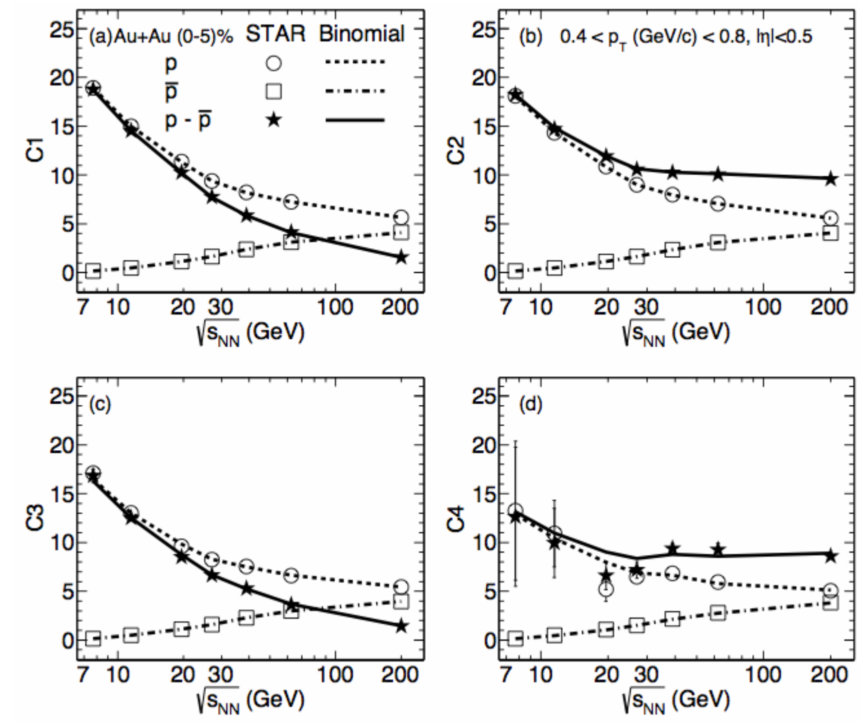

- For Poisson case, the order of cumulant increases the deviations of the data from the Poisson expectation for net-proton and proton increase. Largest deviation is found for C4 at 19.6 and 27 GeV.

- For Binomial case, the agreement persist up to 3rd order. But fails to describe the data for C4 at 19.6 and 27 GeV.

Baseline (II) : UrQMD

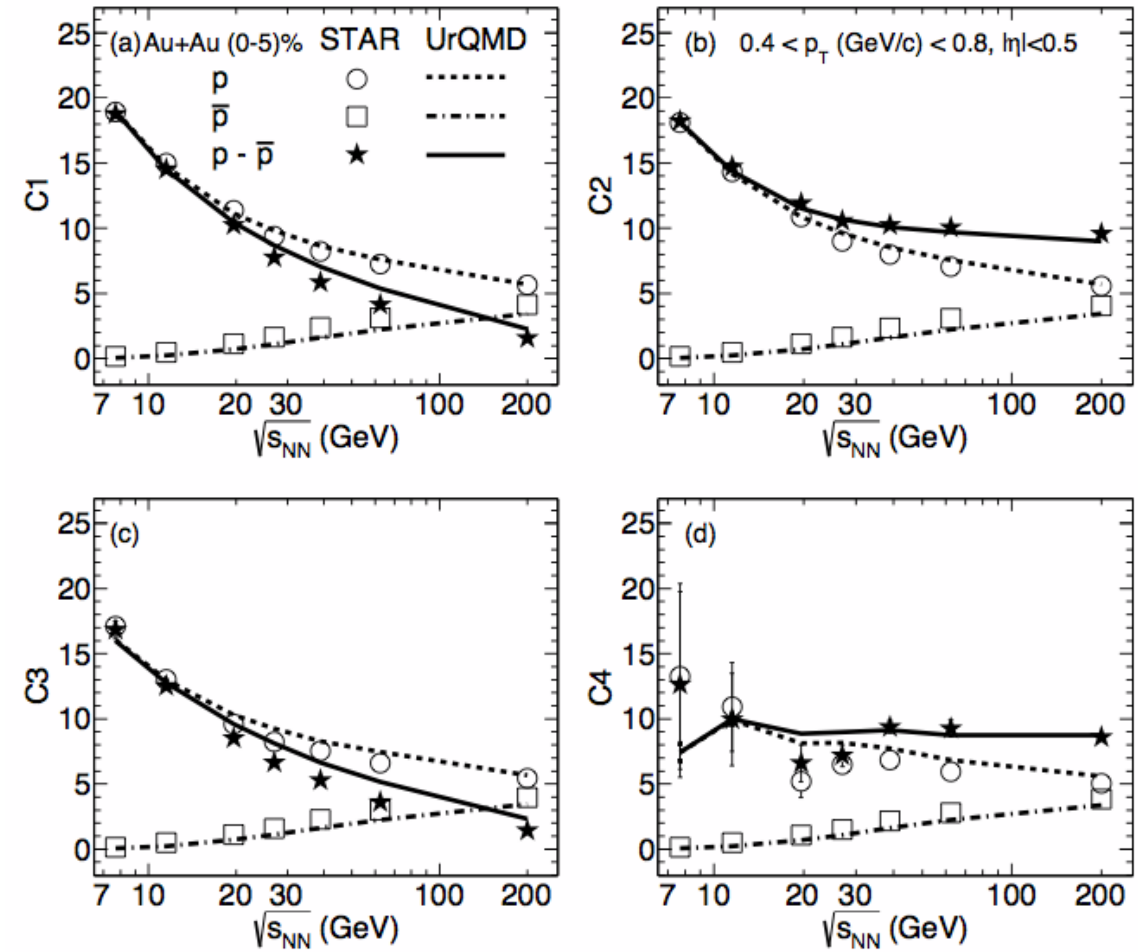

- The anti-proton distributions follow reasonably well the UrQMD expectations.
- The UrQMD model results for higher order cumulants can not explain the measured values at 19.6 and 27 GeV.

Moment Products Vs. UrQMD

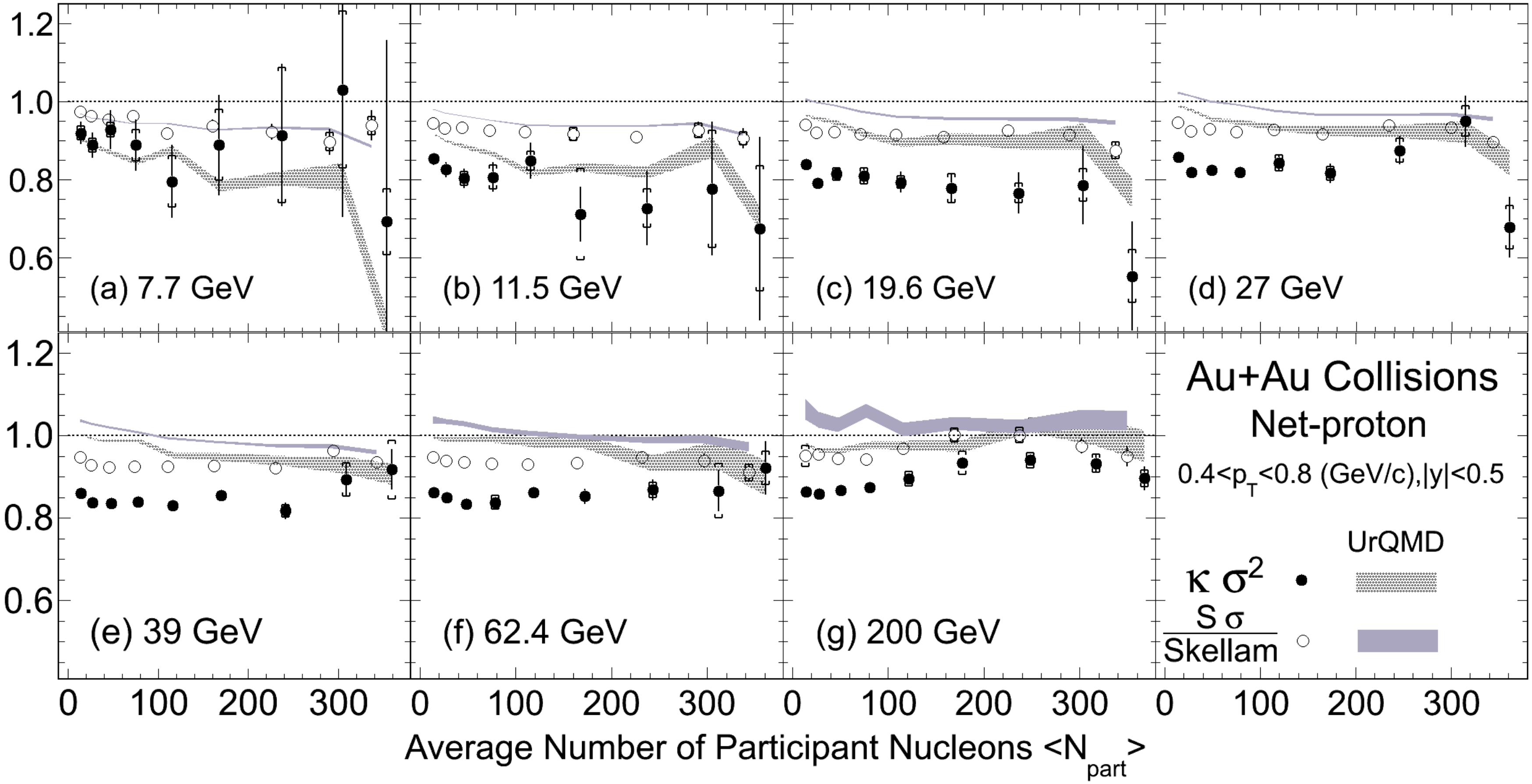

- Good agreement between data and UrQMD for 7.7 GeV and close to data at 11.5 GeV. Disagreement between UrQMD and data for 19.6, 27, 39, 62.4 and 200 GeV.
- For the beam energies of 19.6 and 27 GeV the UrQMD results are higher than the data for most of the centrality presented.

Moments of Net-proton Distribution at RHIC

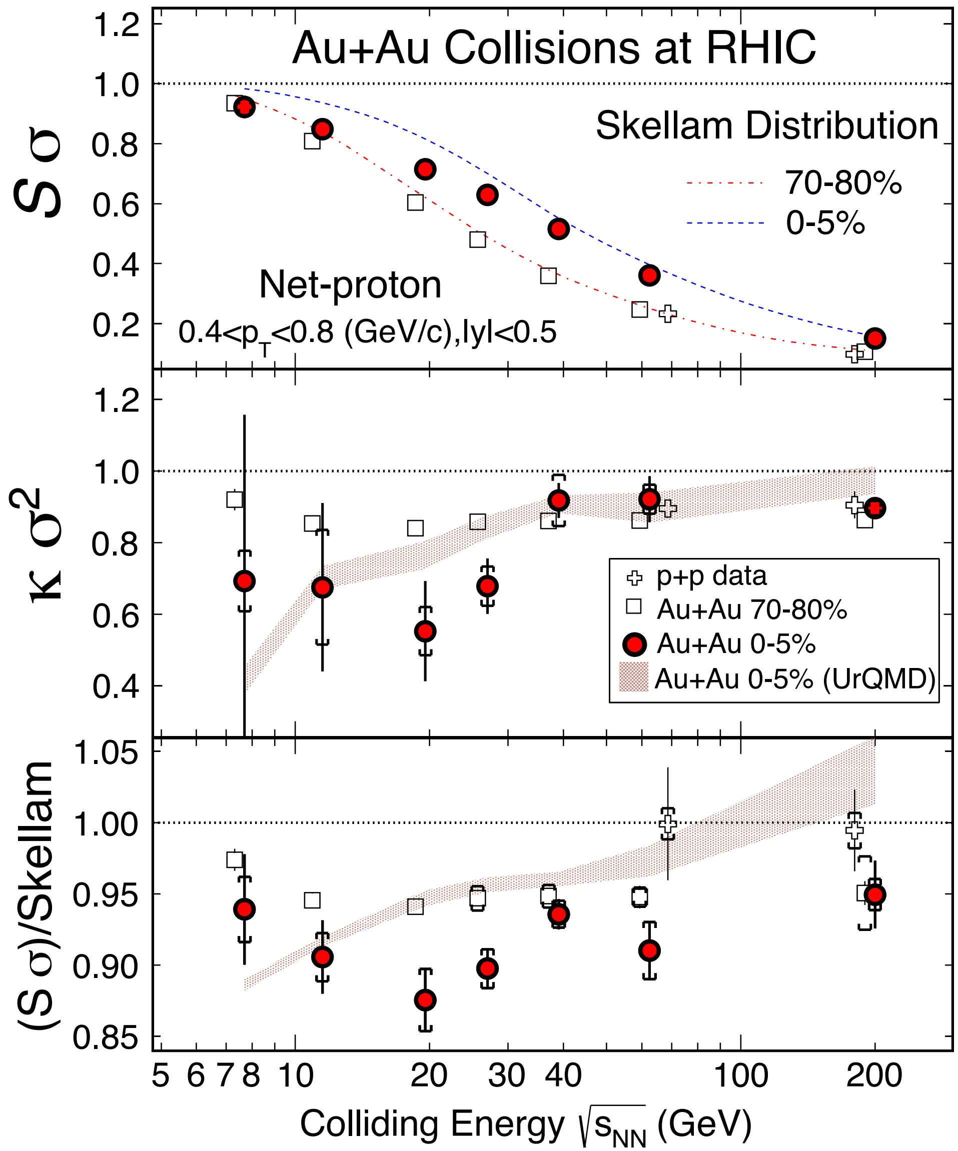

1) All data show deviations below Poisson beyond statistical and systematic errors in the 0-5% most central collisions for $\kappa\sigma^2$ and $S\sigma$ at all energies. Larger deviation at $\sqrt{s_{NN}}$ ~ 20GeV

2) UrQMD model show monotonic behavior in the moment products

3) Higher statistics needed for collisions at $\sqrt{s_{NN}}$ < *20 GeV.* **BES-II is needed**.

4) Compare with QCD based dynamical model.

STAR: Xiaofeng Luo et al.
Phys. Rev. Lett. 112, 032302 (2014)
[arXiv: 1309.5681]

Location of CP: Recent Theory Prediction

Dyson-Schwinger approach (Nf=2+1)

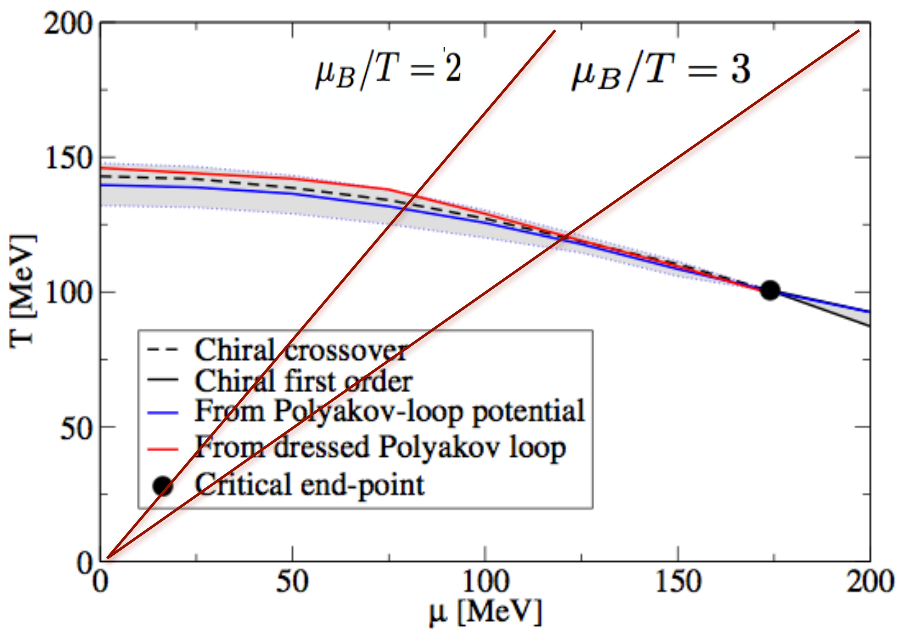

(Quark Chemical Potential)

Lattice QCD (Nf=2+1): Taylor Expansion

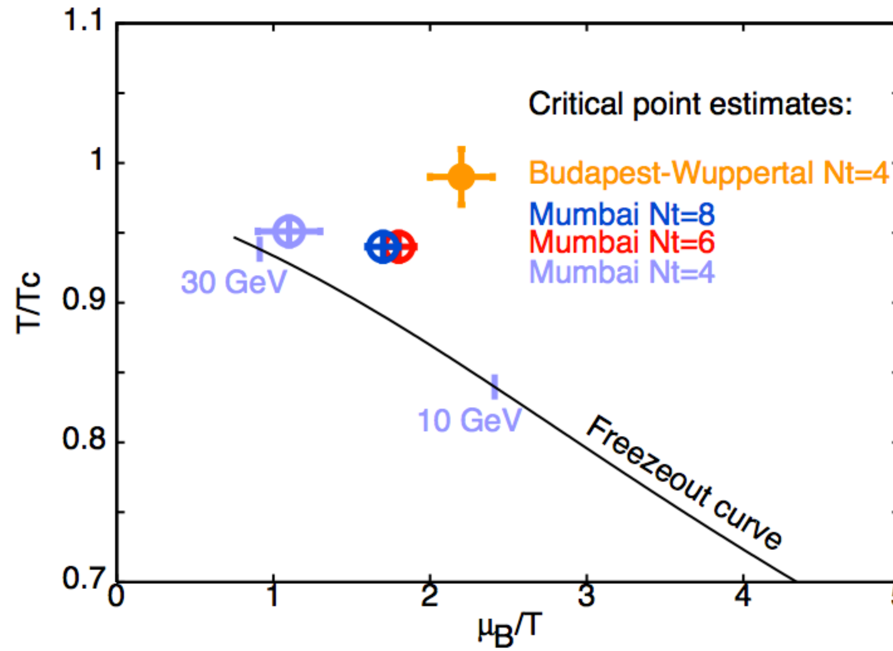

C. S. Fischer, Talk at NFQCD 2013, Japan

S. Gupta, Talk at Lattice 2013, France.

$\mu^E_B/T^E \sim 5$

$\sqrt{s_{NN}}$ ~5 GeV

$\mu^E_B/T^E \sim 1.7$

$\sqrt{s_{NN}}$ ~20 GeV

Different Theory/Method gives very different CP location.

The STAR Upgrades and BES Phase II

- Fine energy scan at $\sqrt{s_{NN}}$ <~ 20 GeV
- Electron cooling will provide increased luminosity ~ 3-10 times
- STAR iTPC upgrade extend mid-rapidity coverage – beneficial to many crucial measurements

e-cooling

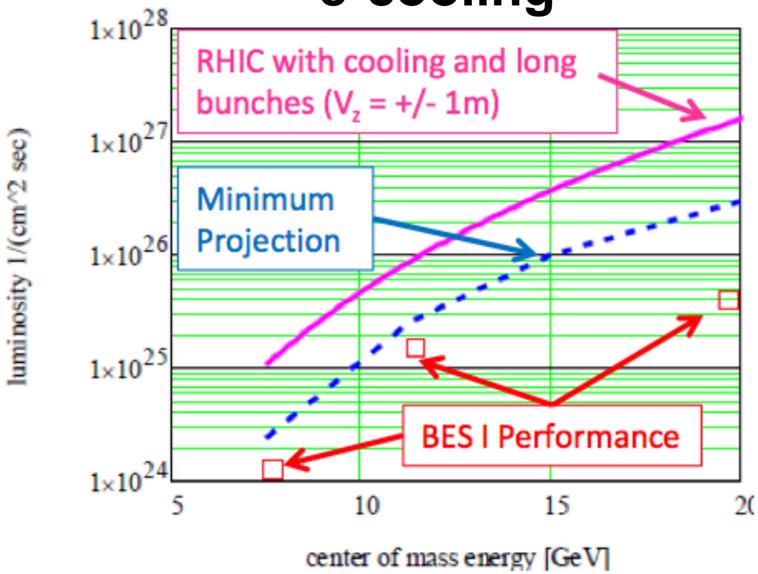

iTPC Upgrade

China : USTC, SDU, SINAP

For moment analysis, iTPC upgrade will provide better efficiency and centrality resolution.

Proposed Statistics for BES-II in BES White Paper

	Collision Energies (GeV):	**7.7**	**11.5**	**14.6**	**19.6**
	Chemical Potenial (MeV):	**420**	**315**	**260**	**205**
	Observables	Millions of Events Needed			
QGP	R_{CP} up to p_T 4.5 GeV	NA	160	92	22
QGP	Elliptic Flow of ϕ meson (v_2)	100	200	200	400
QGP	Local Parity Violation	50	50	50	50
1st P.T.	Directed Flow studies (v_1)	50	100	100	200
1st P.T.	asHBT (proton-proton)	35	50	65	80
C.P.	net-proton kurtosis	80	120	200	400
Chiral	Chiral Trans.- Dileptons	100	230	300	400
	Proposed Number of Events:	**100**	**230**	**300**	**400**

BES Phase II is planned for two 22 cryo-week runs in 2018 and 2019.

Summary

Measurements:

➢ We present the centrality and energy dependence for the first four moments/ cumulants of the net proton multiplicity distributions in Au+Au collisions at RHIC BES-Phase I energies (7.7, 11.5, 19.6, 27, 39, 62.4 and 200 GeV).

Comparisons with Various Baselines and Transport Model:

➢ Deviations below various baselines are observed in Au+Au collision below 39 GeV. Most significant deviation are found around 19.6 and 27 GeV.

➢ Not conclusive yet on searching for the QCD critical point, higher statistics are needed below 27 GeV to get more precise measurement: BES-II (from 2018). Also needs dynamical QCD modeling on the heavy ion collision.

Future Physics Opportunities:

➢ Find the QCD Critical Point：Need efforts from experimentalist and theorist.

➢ Precision measurement of the QGP Properties by comparing the data with the theoretical calculations, such as Lattice QCD.

Thank you !

Back Up Slides

Summary：QCD Phase Diagram

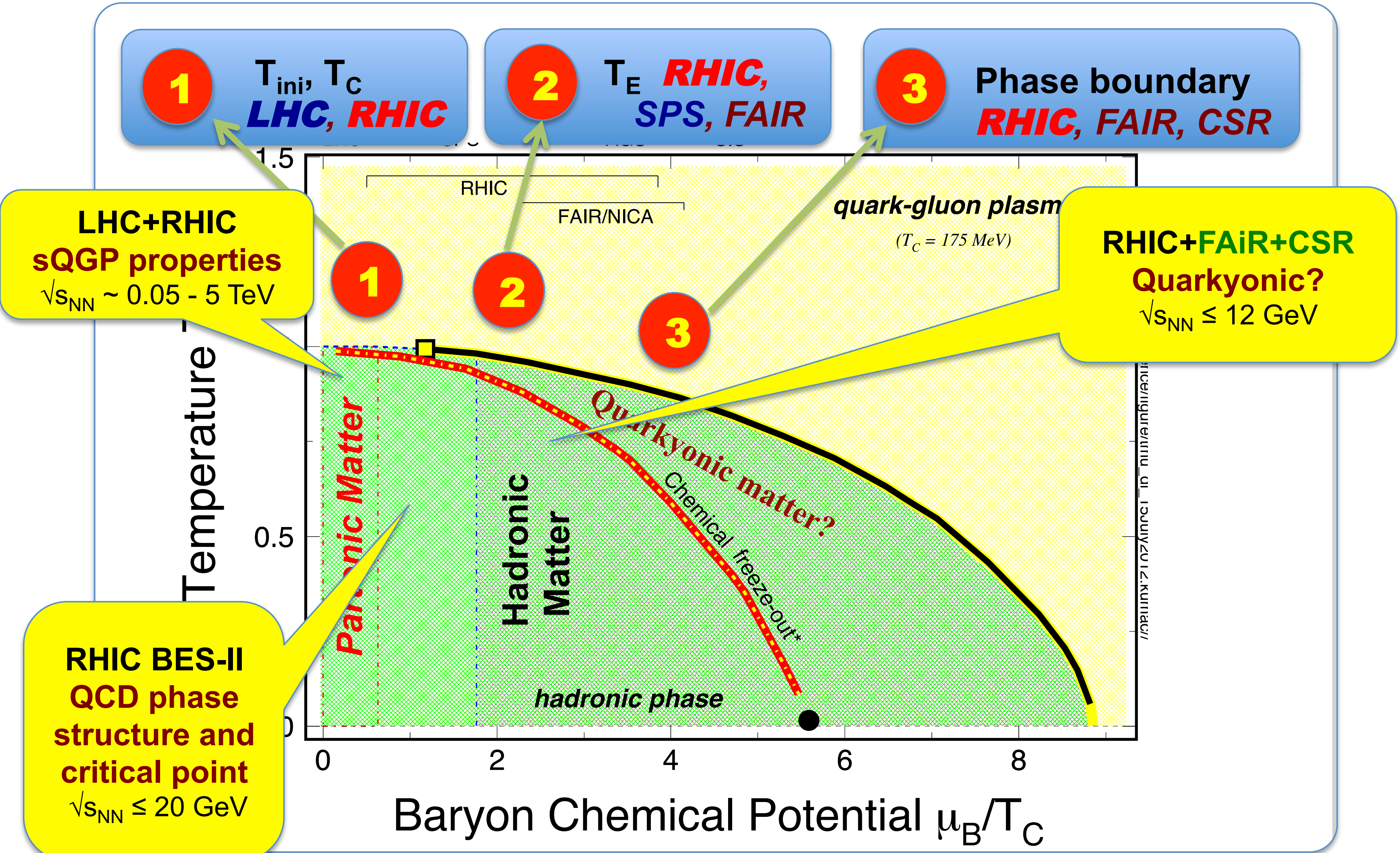

Theoretical Prediction : Critical Point Induced Dip

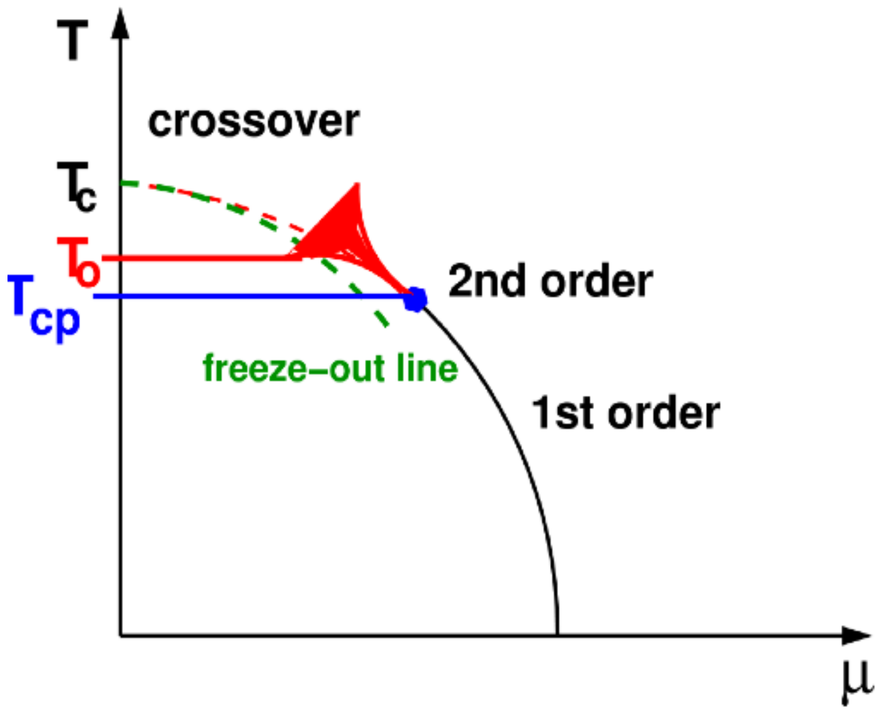

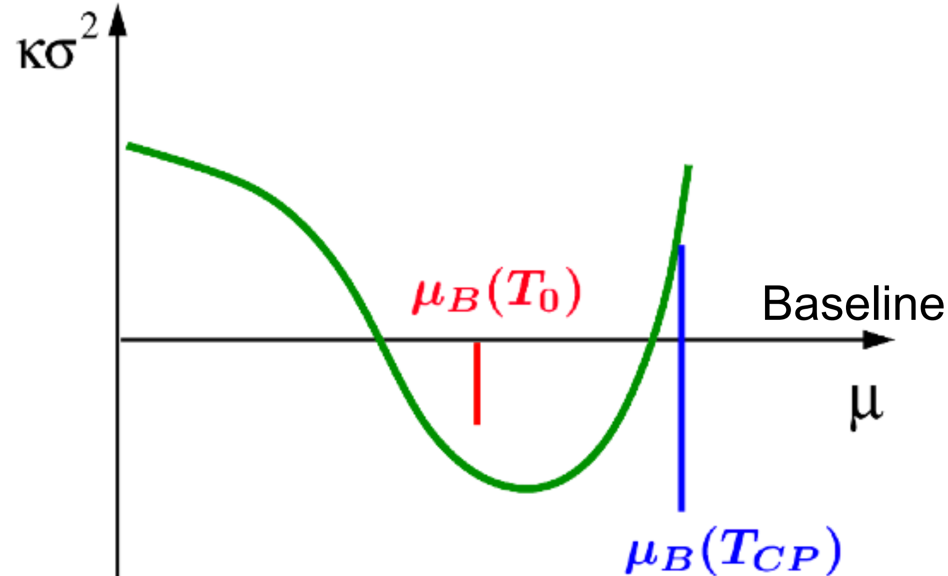

Frithjof Karsch, Talk at NFQCD 2013, Japan.

A dip in the kurtosis*variance is likely to show up on the freeze-out line in the vicinity of a critical endpoint.

see also: Misha Stephanov, Talk at EMMI Workshop 2013, LBNL, US

M. A. Stephanov, Phys. Rev. Lett. 107, 052301 (2011);

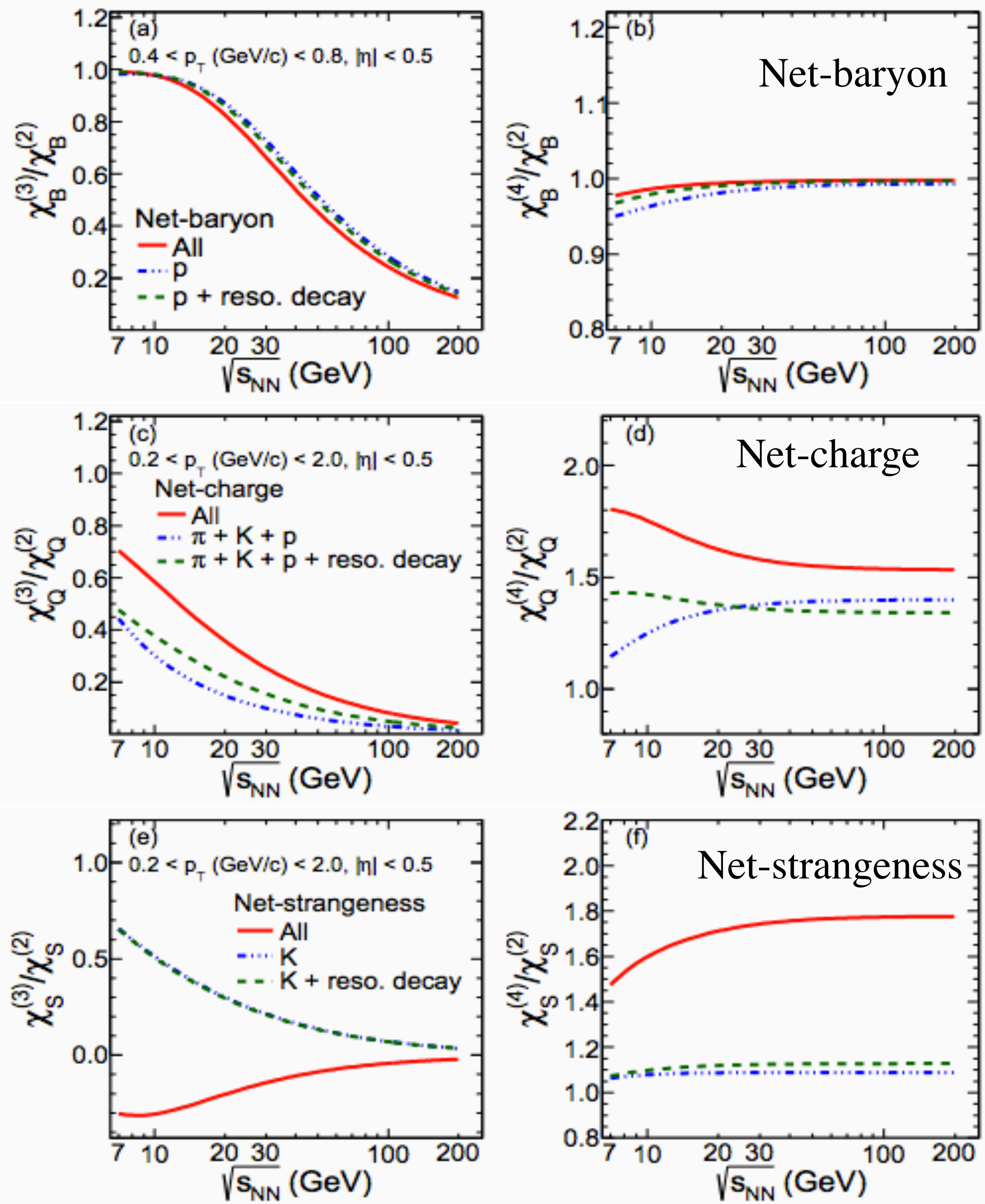

Study by Hadron Resonance Gas Model

arXiv: 1304.7133

- Net-proton is a good approximation of Net-baryon.
- Net-baryon has less decay effect than in net-charge and net-strangeness.
- Particle carrying 2 charge play important role in net-charge.
- Net-kaon is not good approximation of net-strangeness